# Scintillation response of liquid xenon to low energy nuclear recoils

E. Aprile,* K. L. Giboni, P. Majewski, K. Ni, and M. Yamashita
*Physics Department and Astrophysics Laboratory, Columbia University, New York, New York 10027, USA*

R. Hasty, A. Manzur, and D. N. McKinsey
*Department of Physics, Yale University, P.O. Box 208120, New Haven, Connecticut 06520, USA*
(Received 28 March 2005; published 19 October 2005)

Liquid Xenon (LXe) is expected to be an excellent target and detection medium to search for dark matter in the form of Weakly Interacting Massive Particles (WIMPs). We have measured the scintillation efficiency of nuclear recoils with kinetic energy between 10.4 and 56.5 keV relative to that of 122 keV gamma rays from $^{57}$Co. The scintillation yield of 56.5 keV recoils was also measured as a function of applied electric field, and compared to that of gamma rays and alpha particles. The Xe recoils were produced by elastic scattering of 2.4 MeV neutrons in liquid xenon at a variety of scattering angles. The relative scintillation efficiency is $0.130 \pm 0.024$ and $0.227 \pm 0.016$ for the lowest and highest energy recoils, respectively. This is about 15% less than the value predicted by Lindhard, based on nuclear quenching. Our results are in good agreement with more recent theoretical predictions that consider the additional reduction of scintillation yield due to biexcitonic collisions in LXe.

DOI: 10.1103/PhysRevD.72.072006 PACS numbers: 14.60.Pq, 26.65.+t, 29.40.Mc, 95.35.+d

## I. INTRODUCTION

Combined analyses of the latest observational data continue to provide compelling evidence for a significant cold dark matter component in the composition of the Universe[1,2]. In the generic class of Weakly Interacting Massive Particles (WIMPs) that may contribute to the dark matter, the best motivated candidate is the lightest superparticle in supersymmetric (SUSY) Models [3,4]. Its direct detection, via elastic scattering with ordinary nuclei, continues to be the focus of experimental efforts worldwide, using a variety of target nuclei and detector technologies.

Next generation dark matter direct detection experiments, such as XENON[5], are being developed to achieve a substantial improvement in sensitivity by increasing the target mass from the current few kilograms to a few hundred kilograms, while maintaining the excellent background rejection capability demonstrated by cryogenics detectors such as CDMS[6]. Like other experiments being pursued in Europe and Japan[7–9], XENON will use liquid xenon, on the order of 1 tonne, to reach sensitivity to a WIMP scattering cross-section on the order of $10^{-46}$ cm$^2$. An increase in target mass alone is not sufficient, unless the competing backgrounds are eliminated. For XENON, the design goal of 99.5% background rejection efficiency is a result of the simultaneous measurement of the ionization and scintillation signals produced in pure liquid xenon by a WIMP recoil, down to a threshold of 16 keV recoil energy. Event localization in three dimensions and the use of a liquid xenon active shield provide additional discrimination power. In order to establish the background rejection efficiency of LXe for a dark matter search, the absolute ionization and scintillation yields from nuclear recoils has to be precisely known.

Among noble liquids, LXe has the highest scintillation light yield, comparable to that of the best crystal scintillators. The wavelength spectrum of the scintillation photons shows a single peak centered at 178 nm, with a width of approximately 10 nm[10]. The origin of the vacuum ultraviolet scintillation light in liquid xenon is attributed to two separate processes involving excited atoms ($Xe^*$) and ions ($Xe^+$), both produced by ionizing radiation[11]:

$$\begin{aligned} Xe^* + Xe &\rightarrow Xe_2^*, \\ Xe_2^* &\rightarrow 2Xe + h\nu \end{aligned} \tag{1}$$

$$\begin{aligned} Xe^+ + Xe &\rightarrow Xe_2^+, \\ Xe_2^+ + e^- &\rightarrow Xe^{**} + Xe \\ Xe^{**} &\rightarrow Xe^* + \text{heat} \\ Xe^* + Xe &\rightarrow Xe_2^*, \\ Xe_2^* &\rightarrow 2Xe + h\nu \end{aligned} \tag{2}$$

In both Eq. (1) and (2), one exciton or ion produces one ultraviolet photon, $h\nu$, following the creation and radiative decay of an excited dimer, $Xe_2^*$. The lifetimes for the singlet and triplet states of the excited dimer have been measured to be about 4 ns and 22 ns in liquid xenon [12], making LXe the fastest of the noble liquid scintillators. It has also been shown that while these lifetimes do not depend on the density of excited species, the intensity ratio of singlet to triplet states is larger at higher deposited energy density.

Because the excitation density due to nuclear recoils in LXe is higher than that due to electron recoils of the same energy, the scintillation yield is expected to be different.

*Electronic address: age@astro.columbia.edu

 

Knowledge of the ratio of these two scintillation yields is important for the determination of the sensitivity of LXe-based detectors to WIMP dark matter. The ratio has been previously measured [13–16], but data do not cover the lowest recoil energies, which are of interest to sensitive dark matter experiments. Here we report results obtained with a LXe detector exposed to a neutron beam to measure Xe recoil scintillation efficiency in the energy range from 10.4 keV to 56.5 keV. Since some of the LXe dark matter experiments operate with an external electric field to simultaneously detect the scintillation and ionization signals produced by nuclear recoils, we have also measured the scintillation yield as a function of applied electric field up to 4 kV/cm. In the first part of the paper, the experimental apparatus and method is described. Following a presentation of the data, the experimental results are discussed in terms of recent theoretical predictions.

## II. EXPERIMENTAL APPARATUS

The experiments were carried out in the Radiological Research Accelerator Facility at the Columbia Nevis Laboratory. Fast neutrons were produced by bombarding a tritiated target with 3.3 MeV protons. A nearly monoenergetic neutron beam with an average energy of 2.4 MeV in the forward direction was obtained through the T(p, n)$^3$He reaction. The energy spread of the neutrons due to the finite thickness of the tritium target was less than 10% FWHM. A liquid xenon detector was placed 60 cm from the neutron source in the forward direction.

The energy of a xenon recoil can be determined simply from kinematics. The recoil energy $E_r$ transferred to a xenon nucleus when a neutron with energy $E_n$ scatters through an angle $\theta$ is approximately

$$E_r \approx E_n \frac{2M_n M_{\mathrm{Xe}}}{(M_n + M_{\mathrm{Xe}})^2}(1 - \cos\theta), \qquad (3)$$

where $M_n$ is the mass of a neutron and $M_{Xe}$ is the mass of a xenon nucleus. The energy transferred is maximum for back-scattered neutrons. A BC501A liquid scintillator (7.5 cm diameter, 7.5 cm long) with pulse-shape discrimination was used to tag the neutrons scattered in the LXe detector.

The position and size of the neutron detector determine the average and spread of the xenon recoil energy of the tagged events. Data were taken with the center of the BC501A detector at neutron scattering angles of 123, 117, 106, 72, 55 and 44 degrees. The distance between the BC501A and LXe detectors was near 50 cm for all angles. To minimize the chance of direct neutron scattering in the liquid scintillator, the path between the neutron source and the neutron detector was shielded with 30-cm-thick borated polyethylene (5% by weight natural boron). The LXe detector arrangement is shown in Fig. 1. The energy spread due to the finite solid angle of the BC501A neutron detector was approximately 10% FWHM.

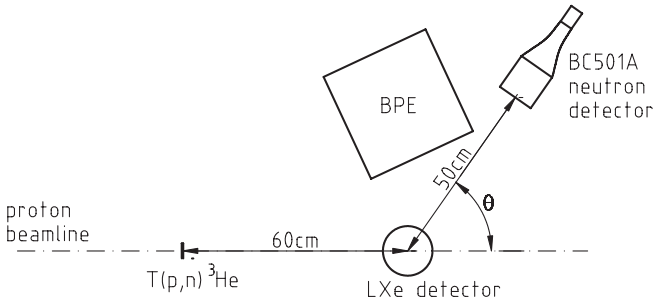


FIG. 1. Schematic view of the detector arrangement used to measure scintillation from nuclear recoils in LXe.

The LXe detector allows a simultaneous measurement of ionization and scintillation signals produced by radiation in its active 21 cm$^3$ volume. A schematic of the LXe detector is shown in Fig. 2. The volume is defined by three transparent wire meshes as cathode, grid and anode of an ionization chamber with a 2 cm drift gap. The scintillation photons are detected by two vacuum ultraviolet (VUV) sensitive, compact metal channel photomultipliers (PMTs), directly coupled to the sensitive LXe volume. To increase light collection, teflon is used as effective VUV reflector[17]. For gain calibration of the PMTs, a blue LED is used. The vessel containing the assembled Teflon structure with meshes and PMTs is enclosed by a vacuum cryostat for thermal insulation. A total of 3.8 kg of high purity Xe gas is condensed in the vessel, cooled by liquid nitrogen [18]. The temperature of the liquid is maintained at $178 \pm 1$ K by controlling the vapor pressure. With continuous vapor phase circulation through a purifier, the concentration of electronegative impurities in the liquid was brought below 1 part per billion, as measured by ionization measurements, triggered on coincidence between the two PMTs. For measurements of the LXe purity and for energy calibration, we used gamma-rays from radioactive sources such as $^{57}$Co and $^{22}$Na, placed directly underneath the cryostat. To demonstrate the excellent light sensitivity of this detector, which enabled us to measure recoils with kinetic energy as low as 10 keV, Fig. 3 shows the scintillation light spectrum of $^{57}$Co gamma-rays at zero electric field. When the 122 keV peak location in the light spectrum is combined with the gain measurement from the single photon peak, the sensitivity is found to be 6 photoelectrons/keV. The measured sensitivity and spectrum are in good agreement with a simulation of the detector response, which takes into account the light collection efficiency and its spatial distribution as described in [19]. For measurements of the light and charge yields of alpha particles in the same detector, also shown in this paper for comparison with nuclear recoils, we used an internal $^{241}$Am source.

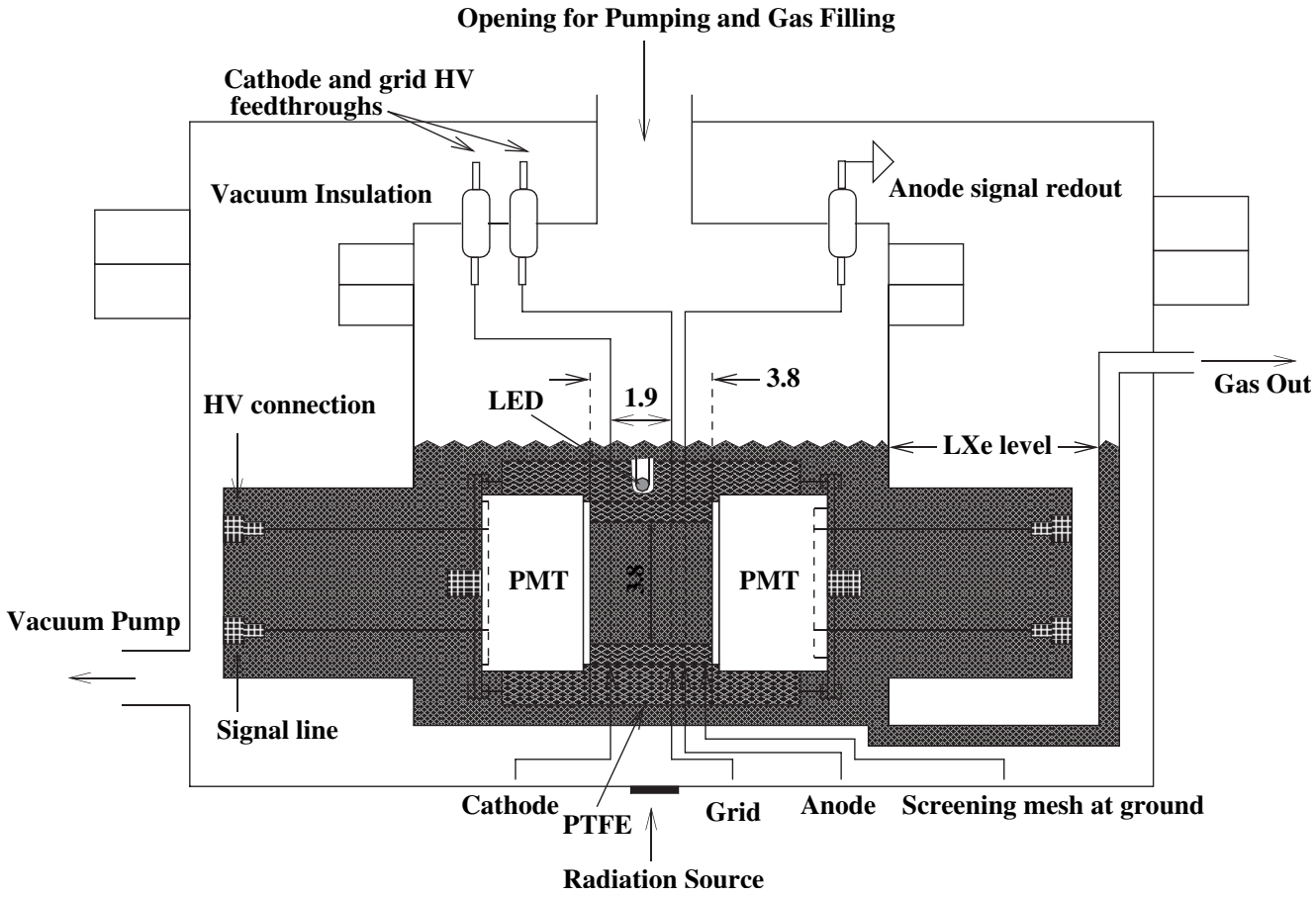


FIG. 2. Schematic view of the LXe detector assembly, with dimensions in cm. The vacuum cryostat surrounding the detector vessel and the cooling system are not shown.

The data acquisition was done with a digital sampling oscilloscope (LeCroy LT374), triggered by NIM coincidence logic. The analog signals from the LXe PMTs and the BC501A PMT were split, with one copy going to a discriminator for each channel. The amplification and discrimination on the LXe channels was set to achieve a single photoelectron threshold. A coincidence unit was used to trigger the oscilloscope on triple coincidences among the two LXe PMTs and the BC501A PMT within 150 ns. The recorded waveforms were transferred to a computer for later analysis.

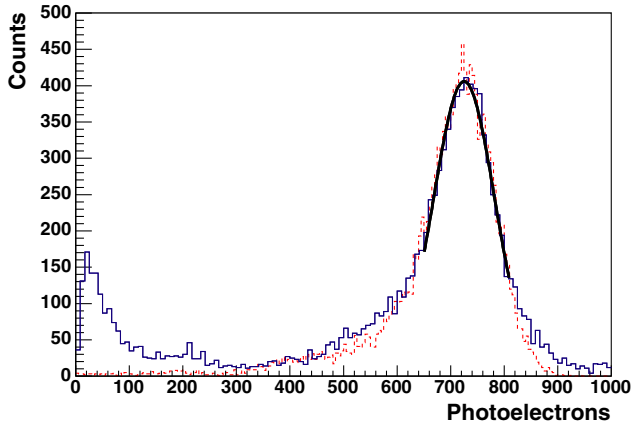


FIG. 3 (color online). $^{57}$Co scintillation light spectrum at zero field (solid line). A fit to the 122 keV peak gives a light yield of about 6 photoelectrons/keV, which is very close to the expected value from simulation (dashed line).

## III. DATA ANALYSIS AND RESULTS

The scintillation efficiency for Xe nuclear recoils is defined as the ratio of the light produced by a nuclear recoil to the light produced by an electron recoil of the same energy. ÊIn practice, the peak in the nuclear recoil spectrum measured at each scattering angle is converted to an electron equivalent energy scale and compared to the expected nuclear recoil energy at that angle. The electron equivalent scale is determined by calibrating the LXe detector with 122 keV gamma rays from $^{57}$Co. In this low energy region, the scintillation response of LXe is not linear, like in many other scintillators[9]. However we chose to calibrate with $^{57}$Co gamma rays in order to compare our data directly to previous works [13,15]. The

expectation value of the nuclear recoil energy is calculated from the geometry of the LXe and BC501A detectors, as in Eq. (1).

The selection of nuclear recoil events is based primarily on time of flight between the LXe and the BC501A detectors. For elastic scattering events where the neutron scatters directly from a Xe nucleus to the BC501A detector, the time of flight is approximately 2 ns for every centimeter of separation. Neutron and gamma coincidences are well separated in the time of flight (ToF) spectrum. Because of the finite size of the detectors, the ToF for neutrons that only scatter once in the active LXe varies by 6 ns. Neutron events in which multiple scattering occurs will generally have a longer ToF than single scattering events, and they also contribute to a tail on the neutron peak in the ToF spectrum. Only events within the first 6 ns of the neutron peak are accepted, and pulse-shape discrimination in the BC501A detector [20] is used to further reduce gamma backgrounds.

The electron equivalent energy spectra for nuclear recoil events with the lowest (10.4 keV) and highest (56.5 keV) recoil energies are shown in Fig. 4, together with the accidental spectrum. The peaks are fit with the sum of a Gaussian and an exponential distribution. The peak location of the Gaussian is divided by the expected recoil energy to determine the scintillation efficiency. ÊThe resulting relative scintillation efficiency, as a function of nuclear recoil energy, is shown in Table I. For recoil energies below 40 keV, where no prior measurements have been reported, the scintillation efficiency drops to 0.13. The errors include both statistical and systematic uncertainties, of similar sizes. The dominant systematic uncertainties are due to the uncertainty in the position of the detectors and the effects of multiple scattering.

The effect of multiple scattering of neutrons in the LXe detector and surrounding materials on the location of the nuclear recoil peak was investigated with a Monte Carlo simulation, using the GEANT4 LHEP-PRECO-HP physics package [21]. A comparison of the simulated recoil spectra including multiple scattering events with the spectra generated with only single scattering events is used to estimate the significance of multiple scattering. These Monte Carlo simulations included a 6 ns ToF cut, which is identical to that used in the analysis of the real data. The effectiveness of the ToF cut for reducing multiple scattering backgrounds is shown in Fig. 5.Ê

TABLE I. The relative scintillation efficiency of Xe nuclear recoils relative to that of gamma rays of the same energy.ÊThe average scattering angle of the neutrons is given by $\theta$. ÊThe average recoil energy of the xenon nucleus is given by $E_r$. Uncertainties include both systematic and statistical contributions.

| $\theta$ (degrees) | $E_r$ (keV) | Relative Efficiency |
|---|---|---|
| 44 | 10.4 | 0.130 ± 0.024 |
| 55 | 15.6 | 0.163 ± 0.023 |
| 72 | 25.6 | 0.167 ± 0.021 |
| 106 | 46.8 | 0.238 ± 0.030 |
| 117 | 53.2 | 0.240 ± 0.019 |
| 123 | 56.5 | 0.227 ± 0.016 |

All the geometries used for the six energies reported in this paper were simulated. The simulations include the LXe detector and its surrounding cryostat, the shielding materials, and the neutron detector. Neutrons with an energy of 2.4 MeV are generated from the location of the neutron source with velocities distributed uniformly over a cone large enough to cover the LXe detector. The expected scattering rates from the simulation are within an order of magnitude of the measured scattering rate.

The multiple scattering has little effect on the location of the peak found by fitting the nuclear recoil spectrum. Simulated spectra including only single scattering events as well as simulated spectra including multiple scattering events are shown in as shown in Fig. 6. For each geometry, the single scattering spectrum is fit with a Gaussian distribution to determine the peak location; the multiple scat-

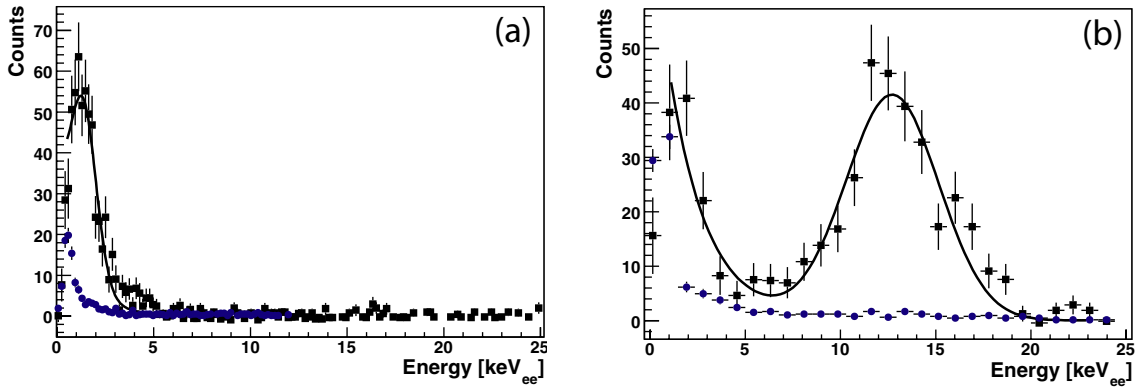


FIG. 4 (color online). The measured LXe scintillation spectra (filled squares) for the (a) 10.4 keV and (b) 56.5 keV nuclear recoil data. The accidental spectrum is shown with filled circles. In both cases the uncertainties are statistical.

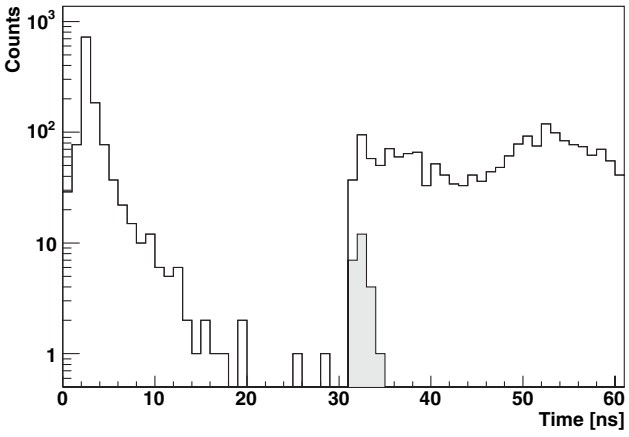


FIG. 5. Simulated ToF data between LXe and BC501A detectors for a scattering angle of 123 degrees. The unshaded histogram is for all single and multiple scattering events, while the shaded histogram is for single scattering events in LXe, followed by scattering in the BC501A detector.

tering spectrum is fit with a Gaussian and an exponential distribution. The simulation shows that multiple scattering events which pass the ToF cut predominantly have one large angle scattering event and one small angle scattering event. This is a consequence of the strongly forward peaked neutron scattering cross section. When the large angle scattering event is in the active region of the LXe, the event shows up in the peak. The difference in the peak location due to these multiple scattering events is less than 5% for every geometry. ÊSimulated spectra for the lowest and highest energy deposition geometries are shown in Fig. 6. It is interesting to note that the expected decreasing efficiency for low energy nuclear recoils has the effect of further reducing the electron equivalent energy for low energy multiple scattering events.

To investigate the dependence of the nuclear recoils scintillation yield on the electric field applied in the liquid xenon, we used the geometry corresponding to 56.5 keV recoils. Because of limited beam availability and having verified that the scintillation yield above 1 kV/cm does not changing appreciably, we concentrated the measurements at fields below 1 kV/cm. At each field, the scintillation efficiency is calculated relative to the scintillation efficiency at zero field, which eliminates uncertainties associated with the determination of the recoil energy. The data are shown in Fig. 7. The error bars include a 10% systematic error due to the variation in the gain of the PMTs

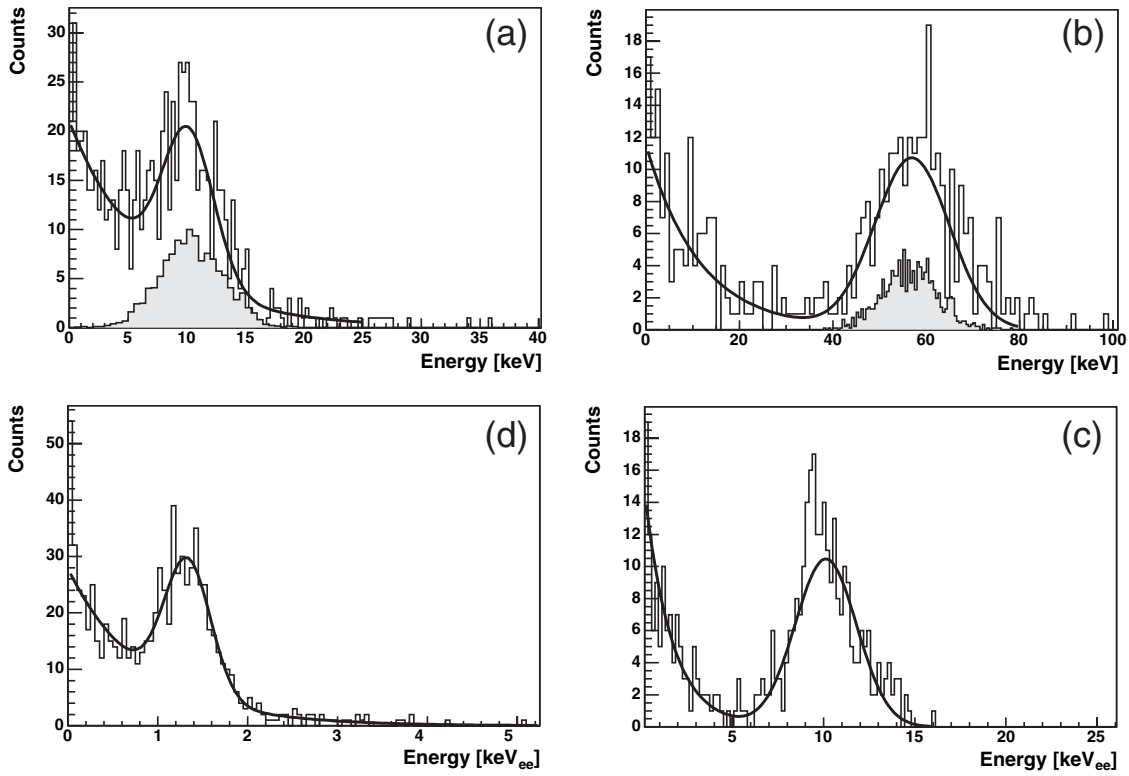


FIG. 6. Monte Carlo simulations of neutron scattering in the LXe detector. (a) Histogram of energy deposition, with $\theta = 44°$ (average energy deposition of 10.4 keV for single elastic scattering events); (b) Histogram of energy deposition, with $\theta = 123°$ (average energy deposition of 56.5 keV for single elastic scattering events); (c) and (d) are the same as (a) and (b), with the energy of each single elastic scattering event multiplied by the theoretically predicted scintillation efficiency [25]. The shaded histogram represents the single scattering results.

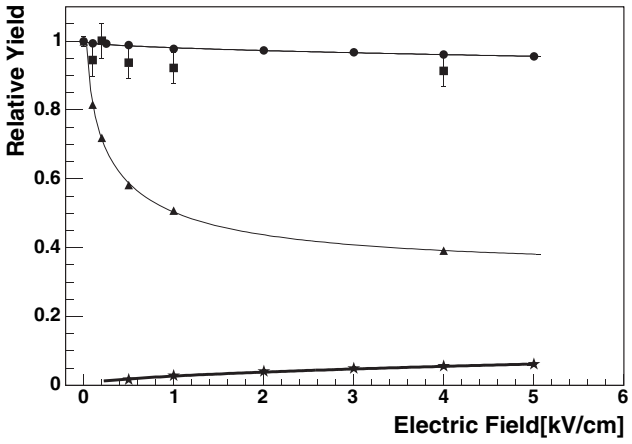


FIG. 7. The LXe scintillation efficiency (squares) for 56.5 keV nuclear recoils, as a function of applied electric field, relative to the zero field efficiency. The uncertainty on the zero field data point is the statistical uncertainty on the location of the peak in the nuclear recoil spectrum, while the uncertainty on the data points with an applied field is dominated by the uncertainty in the gain of the photomultipliers. For comparison, we also show scintillation data obtained with the same detector for 5.5 MeV alpha particles (circles) and for 122 keV gamma-rays (triangles). We also show ionization data for alpha particles (stars).

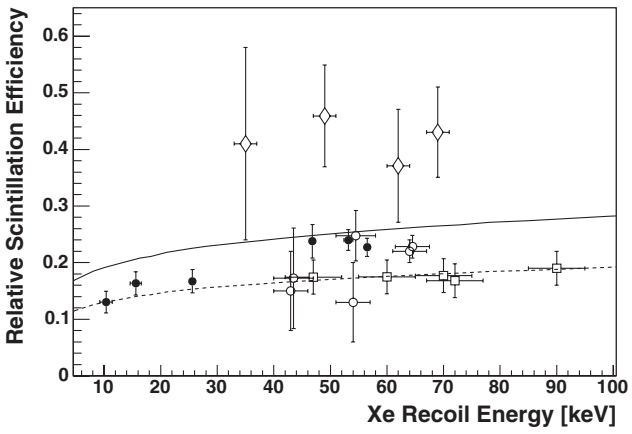


FIG. 8. The relative scintillation efficiency for nuclear recoils as a function of the Xe recoil energy in LXe. The full circles are the data from this experiment. The uncertainties include both statistical and systematic uncertainties. Also shown are measurements by other groups: open circles, squares, and diamonds show the data from Akimov *et al.*[13], Arneodo *et al.* [15], and Bernabei *et al.* [14] respectively. The solid line is from Lindhard [24] and the dotted line is from Hitachi's [25] theoretical model.

immersed in LXe, under prolonged neutron irradiation. The figure also shows the scintillation yield measured with the same detector under 5.5 MeV alpha particles irradiation and under 122 keV gamma-rays irradiation. The ionization yield for alpha particles is shown as well. As previously measured in LXe [22,23], the strong recombination rate along alpha particle tracks is such that only about 6% of the liberated charges are collected even at 5 kV/cm, whereas more than 90% are collected for 1 MeV electrons at the same field.

## IV. INTERPRETATION OF RESULTS

For recoils with energy in the range of 10.4 to 56. keV, we find the relative scintillation efficiency to be in the range 0.13 to 0.23. For the lowest recoil energies, our data are the first reported, to our knowledge. Compared to the scintillation yield due to electron or alpha particle excitation, the scintillation yield due to nuclear recoil excitation is significantly reduced. Our results are shown in Fig. 8, along with previous measurements by other groups [13–16]. The predicted curves from theoretical models from Lindhard [24] and Hitachi[25] are also shown as solid and dotted lines, respectively. The scintillation efficiency of LXe is about 15% less than the Lindhard prediction. Hitachi explains this difference by estimating the additional loss in scintillation yield that results from the higher excitation density of nuclear recoils.

Rapid recombination in LXe under high Linear Energy Transfer (LET) excitation[12,26] provides a mechanism for reducing the scintillation yield of nuclear recoils in addition to that of nuclear quenching treated by Lindhard. In order to estimate the total scintillation yield, Hitachi considers biexcitonic collisions, or collisions between two ''free'' excitons that emit an electron with a kinetic energy close to the difference between twice the excitation energy $E_{ex}$ and the band-gap energy $E_g$ (i.e. $2E_{ex}$–$E_g$):

$$\hat{\mathrm{E}}\,\mathrm{Xe}^* + \mathrm{Xe}^* \rightarrow \mathrm{Xe} + \mathrm{Xe}^+ + \mathrm{e}^-$$

The electron then loses its kinetic energy very rapidly before recombination. This process reduces the number of excitons available for VUV photons since it requires two excitons to eventually produce one photon. It is therefore considered the main mechanism responsible for the reduction of the total scintillation yield in LXe under irradiation by nuclear recoils. As shown in Fig. 8, our data are in good agreement with the Hitachi prediction.

Simultaneous measurements of scintillation and ionization signals from nuclear and electron recoils in LXe are expected to provide a powerful background discrimination for a LXe dark matter detector such as XENON. Charge collection by an external field is expected to be difficult for nuclear recoils in LXe, since the initial radial distribution of excited species in a Xe recoil track is estimated to be similar to the track core of an alpha particle [12]. This similarity is also implied by our data on the electric field dependence of the scintillation yield for 56.5 keV Xe recoil, which is not very different than that of alpha particles in LXe (see Fig. 7). Even at the highest field of 4 kV/cm, recombination is very strong and the light yield is suppressed by less than 5%. No satisfactory theory exists

for the ionization yield $Q(E)/Q(0)$ due to heavy ions as a function of applied field E in noble liquids. Here $Q(0)$ is the charge produced by a particle in units of electrons, which for the case of recoil ions can be written as $Q(0) = q_{nc}E_r/W$, with $W$ the average energy to produce an electron and ion pair [27] and $q_{nc}$ the Lindhard nuclear quenching factor [24]. For the case of LXe, measurements of ionization yield for heavily ionizing particles are limited to alpha particles. The alpha data for electric fields in the typical range of 1–10 kV/cm are well parametrized by an empirical form of the type $Q(E)/Q(0) = aE^b$, with $E$ in kV/cm. The result of a fit with this function to our 5.5 MeV alpha ionization data shown in Fig. 7 gives $a = 0.021 \pm 0.004$ and $b = 0.52 \pm 0.14$, consistent with values obtained from fitting previous alpha ionization data in LXe [28]. Using the fitted parameters, we would expect at least 50 ionization electrons to be collected at a field of 5 kV/cm for 56.5 keV nuclear recoils in LXe. We note that on the basis of the Bragg-like curve and the electronic LET, the ionization density along a Xe recoil track in LXe increases as the recoil energy increases[25]. This suggests that charge collection at a given field becomes more difficult as the energy of the recoil increases. A direct measurement is needed for the ionization yield of Xe recoils in LXe and we are preparing a dedicated dual phase (liquid/gas) Xe detector to carry out such measurements, as a function of recoil energy and applied electric field.

## V. SUMMARY

In summary, we have measured the scintillation efficiency of Xe recoils relative to that of 122 keV gamma-rays, using a LXe detector with PMTs operating in the liquid for enhanced light collection. The high photoelectron yield of 6 photoelectrons/keV has allowed us to measure for the first time the scintillation efficiency of Xe recoils with energy as low as 10.4 keV. For Xe recoils of 56.5 keV, the dependence of the scintillation yield on the applied electric field has also been measured and found to be similar to that of alpha particles. The scintillation response for low energy nuclear recoils is of great relevance to LXe dark matter searches designed to probe the lowest spin-independent WIMP-nucleon cross-section predictions.

## ACKNOWLEDGMENTS

We express our gratitude to Dr. Steve Marino of the Columbia RARAF facility for the beam time and his support throughout the measurements. We would also like to thank Dr. A. Hitachi for valuable discussions and comments. This work was supported by a grant from the National Science Foundation to the Columbia Astrophysics Laboratory (Grant No. PHY-02-01740) for the development of the XENON Dark Matter Project.

[1] D. N. Spergel *et al.*, Astrophys. J. Suppl. Ser. **148**, 175 (2003).
[2] W. Freedman and M. Turner, Rev. Mod. Phys. **75**, 1433 (2003).
[3] M. W. Goodman and E. Witten, Phys. Rev. D **31**, 3059 (1985).
[4] G. Jungman, M. Kamionkowski, and K. Griest, Phys. Rep. **267**, 195 (1996).
[5] E. Aprile *et al.* (XENON Collaboration), Nucl. Phys. B, Proc. Suppl. **138**, 156 (2005).
[6] CDMS collaboration, Phys. Rev. Lett. **93**, 211301 (2004).
[7] D. B. Cline *et al.*, Nucl. Phys. B, Proc. Suppl. **124**, 229 (2003).
[8] Y. Suzuki, hep-ph/0008296.
[9] M. Yamashita *et al.*,Astropart. Phys. **20**, 79 (2003).
[10] J. Jortner, *et al.*,J. Chem. Phys. **42**, 4250 (1965).
[11] S. Kubota *et al.*, Phys. Rev. B **17**, 2762 (1978).
[12] A. Hitachi *et al.*, Phys. Rev. B **27**, 5279 (1983).
[13] D. Akimov *et al.*, Phys. Lett. B **524**, 245 (2002).
[14] R. Bernabei *et al.* Eur. Phys. J. **C11**, 1 (2001).
[15] F. Arneodo *et al.*, Nucl. Instrum. Methods Phys. Res., Sect. A **449**, 147 (2000).
[16] R. Bernabei *et al.*, Phys. Lett. B **389**, 757 (1996).
[17] M. Yamashita *et al.*, Nucl. Inst. and Meth. A **535**, 692 (2004).
[18] E. Aprile *et al.*, Nucl. Inst. and Meth. A **480**, 636 (2002).
[19] E. Aprile *et al.* (to be published).
[20] S. Marrone *et al.*, Nucl. Inst. and Meth. A **490**, 299 (2002).
[21] S. Agostinelli *et al.*, Nucl. Inst. and Meth. A **506**, 250 (2003).
[22] E. Aprile, R. Mukherjee, and M. Suzuki, IEEE Trans. Nucl. Sci. **37**, 553 (1990).
[23] E. Aprile, R. Mukherjee, and M. Suzuki, Nucl. Inst. and Meth. A **302**, 177 (1991).
[24] J. Lindhard, Mat. Fys. Medd. K. Dan. Vidensk. Selsk. **33**, 1 (1963).
[25] A. Hitachi, in *Proceedings of the Fourth International Workshop, York, UK, 2002*, edited by Neil J. C. Spooner and Vitaly Kudryavtsev (University of Sheffield, United Kingdom, 2003), p. 357; in *5th International Workshop on the Identification of Dark Matter, IDM2004, Edinburgh, Scotland, 2004* (unpublished).
[26] A. Hitachi, T. Doke, and A. Mozumder, Phys. Rev. B **46**, 011463 (1992).
[27] T. Doke *et al.*, Jpn. J. Appl. Phys. **41**, 1538 (2002).
[28] H. Ichinose *et al.*, Nucl. Inst. and Meth. A **305**, 111 (1991).